https://doi.org/10.5194/essd-2026-469
Preprint. Discussion started: 10 July 2026

Open Access Earth System Science Data Discussions

Dataset of daily vertical displacements observed by GPS between 1994 and 2023 for hydrogeodetic studies over Europe

Anna Klos[1,2], Jürgen Kusche[2], Anne Springer[2], Artur Lenczuk[1], Yorck Ewerdwalbesloh[2], Christian Mielke[2], Susanna Werth[3,4], Jan Mikocki[1], Kinga Klos[1], Jakub Rados[1], Malgorzata Sieczak[1], Janusz Bogusz[1]

[1]Military University of Technology, Warsaw, Poland
[2]University of Bonn, Bonn, Germany
[3]Virginia Tech, Blacksburg, USA
[4]United Nations University Institute for Water, Environment and Health, Hamilton, ON, Canada

Correspondence to: Anna Klos (anna.klos@wat.edu.pl)

Abstract. Europe is currently the fastest-warming continent in the world, and it has experienced frequent and severe weather events, which have led to extensive droughts and floods, with consequences for ecosystems, health, economy, and other sectors. During the past two decades, these hydrological extremes have been quantified using Terrestrial Water Storage (TWS) changes obtained from the Gravity Recovery and Climate Experiment (GRACE) mission and its successor GRACE Follow-On. Unfortunately, GRACE/-FO-derived TWS changes do not have sufficient temporal and spatial resolutions for detailed analysis of sub-regional patterns or sub-monthly TWS changes over Europe, e.g., at the Eurostat NUTS 2 or 3 level. We suggest that both spatial and temporal resolutions could be enhanced in the future by using displacement time series observed at more than 6,000 permanent Global Positioning System (GPS) European stations. However, to turn this network into an observing system for TWS anomalies, GPS displacements must be carefully prepared in advance, and no useful dataset is available to our knowledge. Here we provide, for the first time, a quality-controlled dataset of long daily vertical displacement time series observed at 4,443 GPS antennas in Europe and surrounding regions between 1994 and 2023, after preprocessing and preselection to remove displacements seemingly unrelated to hydrospheric loading. We classify stations that pass our procedure as reference time series (benchmark datasets) with respect to hydrospheric changes. Three benchmark datasets are provided for use at different temporal scales: long-term (>1.1 years), seasonal (from 4 months to 1.4 years) and short-term (from 2 days to 5 months), even for the period of 8 years prior to GRACE (Klos and Bogusz, 2026). We show in this study that the displacements recorded by GPS stations included in the benchmark datasets (1) are to a great extent coherent with hydrological models, reflect accumulated precipitation records, and clearly reflect the influence of climate modes, (2) are mutually highly consistent on a regional scale and also consistent with the displacements determined by the InSAR (Interferometric Synthetic Aperture Radar) technique, (3) allow for the estimation of high-resolution TWS changes at all three temporal scales well, which matches closely with GRACE and ERA5-Land, potentially allowing for a better understanding of regional changes in the European hydrosphere.

1 Introduction

Terrestrial Water Storage (TWS) changes are estimated with great success using observations from the Gravity Recovery and Climate Experiment (GRACE) satellite mission, which operated from 2002 until 2017, and then, after a gap of almost a year, from its follow-up mission GRACE Follow-On (Tapley et al., 2004; Chen et al., 2022). For clarity, we abbreviate both missions as GRACE throughout the manuscript. Despite its many advantages, such as providing global coverage (Eicker et al., 2016; Tapley et al., 2019; Humphrey et al., 2023), the GRACE mission also has significant limitations in determining TWS changes, such as a temporal resolution of one month with many gaps in later years, and a spatial resolution of approximately 300 km (Tapley et al., 2004).

https://doi.org/10.5194/essd-2026-469
Preprint. Discussion started: 10 July 2026

TWS changes can alternatively be estimated from displacements observed by the Global Navigation Satellite System (GNSS) permanent stations, with Global Positioning System (GPS) still being the most used system. Several authors suggested applying inversion procedures (or reverse modelling), which uses the Green's functions to relate the Earth's crustal elastic response to surface loading (e.g., Wahr et al., 2013; Argus et al., 2014). Compared to GRACE, the use of GPS displacements to determine TWS changes suggests several benefits (White et al., 2022). Firstly, since time series of displacements have been available since 1994, the resulting TWS changes can be obtained for the same period, long before the GRACE mission began. Secondly, our growing understanding of noise present in displacement time series (e.g., Gobron et al., 2021, 2024) allows us to obtain a series of daily displacements with low noise levels, thereby improving the temporal resolution of the resulting TWS changes (Han and Razeghi, 2017; Jiang et al., 2021). Finally, with the current number of GPS stations available worldwide, the spatial resolution of the resulting TWS changes can reach 50 km for regions with dense networks of permanent stations, such as North America (Argus et al., 2014; Fu et al., 2015; Ferreira et al., 2018). Given all these benefits, long time series of daily GPS displacements are currently used to study changes in TWS and its components at different temporal scales, with time series longer than those derived from GRACE (Ouellette et al., 2013; Adusumilli et al., 2019; Yin et al., 2020; Larochelle et al., 2022), improve spatial resolution of TWS changes (Argus et al., 2014), estimate daily hydrospheric loading during hydrometeorological events (Milliner et al., 2018; Zhan et al., 2021; Jiang et al., 2021), monitor drought conditions (Chew and Small, 2014; Ferreira et al., 2018; Jiang et al., 2021; Lenczuk et al., 2024; Young et al., 2024), validate TWS changes (Richter et al., 2021; Gerdener et al., 2023a), improve estimates of TWS by assimilation into land surface models (Yin et al., 2021) and, finally, integrate with other geodetic techniques, such as GRACE or InSAR (Interferometric Synthetic Aperture Radar) (Adusumilli et al., 2019; Carlson et al., 2022, 2024). Unfortunately, a manual pre-analysis, and pre-selection is necessary for each station individually to identify and exclude anomalous GPS displacements for which either technique-specific errors or other physical processes (Ray et al., 2008; Lei et al., 2020; Gruszczynski et al., 2018; Langbein and Svarc, 2019) dominate over hydrospheric loading signal before TWS can be reliably inferred. Manual cleaning of GPS displacements is very tedious, and time-consuming, especially with a large number of GPS stations, and requires considerable experience. It is highly prone to errors and to analyst bias and subjective judgments. Initial pre-selection is currently based on a comparison of the amplitude and phase of annual signals between GPS-observed and GRACE-derived displacements (Lau et al., 2020; Argus et al., 2017; Jiang et al., 2017), which favors annual signals, giving other and often more important temporal scales much less importance. Since we believe that some time series are mutually consistent with others at some temporal scales and not at another, we use the methodology for identifying GPS stations sensitive to hydrosphere at various temporal scales (Klos et al., 2023), and provide, for the first time, a unique, quality-controlled benchmark dataset of daily GPS-observed vertical displacements across Europe. We compile three benchmark datasets for use at temporal scales: long-term (>1.1 years), seasonal (from 4 months to 1.4 years), and short-term (from 2 days to 5 months). Our benchmark datasets are provided for Europe, which is currently the fastest-warming continent in the world (see Copernicus Climate Change Service), and where extreme meteorological events have already caused droughts and floods with wide consequences in sectors such as transport, health, agriculture, industry, hydropower, and others. Yet hydrological modelling and prediction exhibit significant shortcomings as various comparisons to the GRACE-derived TWS changes have shown in recent years (Scanlon et al., 2016, 2018). We argue that GPS displacements can significantly improve the estimation of TWS changes over GRACE, and that this has potential for further use in hydrological model evaluation or the assimilation of TWS maps in operational frameworks, e.g. in drought monitoring (Young et al., 2024). There are over 6,000 permanent GPS stations operating in Europe, with incredible spatial coverage that can guarantee high-resolution spatial analysis. The resulting dataset of daily GPS-observed vertical displacements can be used directly by several communities to estimate daily TWS changes in Europe at three temporal scales. We caution, however, that at the long-term temporal scale, we provide de-trended time series. We provide estimated trends along with a benchmark dataset, but caution that particular care should be taken when using them

https://doi.org/10.5194/essd-2026-469
Preprint. Discussion started: 10 July 2026

in hydrological applications. This is because trends are extremely sensitive to the length of the time series from which they are determined, and the lengths of GPS displacement records vary depending on the station.

This paper is organized as follows. In section 2, we present GPS-observed displacements and their detailed pre-processing, along with the method of classifying GPS stations as hydrogeodetic benchmark datasets. We also introduce all external datasets we use for validation and comparisons. In section 3, we perform quantitative and qualitative validation of our benchmark datasets and, finally, we use our benchmark dataset to model TWS changes for the Seine River basin as an example for a region under anthropogenic water stress. The article concludes with a summary, provided in section 4.

2 Data and methods

2.1 GPS position time series

We retrieve a set of daily X, Y, and Z geocentric coordinates from the Nevada Geodetic Laboratory (NGL; Blewitt et al., 2018), which processes GPS observations using GipsyX Version 1.0 in Precise Point Positioning (PPP; Zumberge et al., 1997) mode under the following assumptions. Wet and dry parts of the troposphere are modeled using a priori estimates from the Vienna Mapping Function (VMF1) with nominal gradients set to zero. Zenith delays and gradients are estimated as a random walk process every 5 minutes. The first-order ionospheric effect is accounted for by using carrier-phase and pseudo-range combinations. The second-order ionospheric effect is modeled using IONEX data from IGRF12 (International Geomagnetic Reference Field). Phase center offsets are adopted from 'igs14_wwww.pcm' file, and the phase center variations are computed with respect to 'igs14_www.atx' file. Solid Earth tide and pole tide are removed using IERS2010 Conventions, while preserving the permanent tide. Non-tidal loading models are not applied. More details on the NGL processing can be found through the NGL website (https://geodesy.unr.edu/gps/ngl.acn.txt).

We transform daily changes in XYZ coordinates from the txyz2 files for 6,259 GPS stations in Europe (cf. Figure 3 in Hammond et al., 2021), during 1994-2023, to an ellipsoidal topocentric system North, East, and Up, and then use vertical displacements. We then employ the effective completeness (EC) parameter introduced by Kreemer and Blewitt (2021), to retrieve an effective representation of the availability of GPS displacements over time, relative to the record length:

$$EC = \sqrt{(N-G)M} \,/\, T \tag{1}$$

where N is the total number of days within the considered displacement time series, G is the number of days of the largest data gap, M is the number of days with data, and T is the number of days between 1994 and 2023. Figure 1 presents the effective completeness of GPS displacements for the European set of stations, which varies between 0 (for no data) and 1 (for fully complete). For most GPS stations, the EC falls between 0.1 and 0.5. For 41 stations, the EC exceeds 0.9. These values indicate that GPS observation availability in Europe during the period 1994–2023 is good, significantly higher than the availability of observations, for example, at stations located in Africa, but comparable to the values recorded for stations in North America (Hammond et al., 2021).

https://doi.org/10.5194/essd-2026-469
Preprint. Discussion started: 10 July 2026

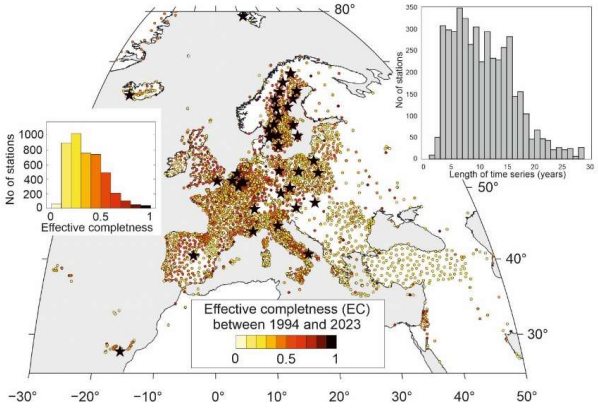

Figure 1: Network of GPS stations in Europe. Left: effective completeness of GPS displacements between 1994 and 2023. Stations with effective completeness higher than 0.9 are marked with black stars. Right: histogram of the length of all GPS time series in years.

2.2 Vertical displacements predicted from the hydrological model

To classify GPS stations as benchmark datasets, we compare the GPS-observed vertical displacements with vertical displacements predicted by a hydrological model. For this task, we make use of simulations with the eCLM fork of the Community Land Model 5.0 (CLM5), the land surface component of CESM. eCLM is implemented within the Terrestrial Systems Modeling Platform version 2 (TSMP2, Poll et al., 2025) and simulates key hydrospheric processes such as infiltration, runoff, canopy interception, and snow dynamics, and includes a groundwater layer. Subgrid-scale heterogeneity is represented by a hierarchical structure of land units, columns, and patches that distinguish surface types including vegetation, lakes, and cropland. Water storage is simulated in up to 20 soil layers reaching 8.03 m depth and includes canopy, surface water, snow, soil liquid water, and soil ice; TWS is diagnosed as the sum of these components. eCLM is applied over Europe on the Euro-CORDEX EUR-11 grid (0.11°, ~12.5 km) with hourly time steps, using static land surface and soil parameters from SoilGrids, ERA5 (the fifth generation of European ReAnalysis) atmospheric forcing, and land cover from the Global Land Cover 2000 dataset. Compared to global hydrological models and GRACE observations, eCLM provides higher temporal resolution and a representation of the diurnal cycle, higher spatial resolution, and a detailed representation of soil layers, vegetation, and land cover heterogeneity, making it particularly suitable for capturing regional hydrological variability in Europe. Compared to earlier versions CLM3.5, 4.0 and 4.5, CLM5.0 and eCLM add many process representations and improvements that render this model particularly suitable for comparison to, and integration with GRACE data (Ewerdwalbesloh et al., 2026).

We use hourly TWS time series from the eCLM hydrological model for 2003-2022 period (Springer et al., 2024) and average these samples into daily samples, in agreement with the GPS-observed displacements. To compute vertical displacements at a European set of GPS locations, we use these daily averages with a spatial resolution of 12 km and represent them as spherical harmonic coefficients to degree and order 360, which corresponds to approximately 50 km spatial resolution. We apply load Love numbers derived from the Gutenberg-Bullen A Earth model and methodology given by Farrell (1972) to estimate the vertical displacements for GPS locations. We also tested further increases in resolution derived by the higher spherical harmonic representation, but this led to changes in vertical displacements of less than 1 mm.

2.3 Detailed pre-processing of GPS-observed displacement time series and benchmarking

We perform a detailed pre-processing procedure, identical to the ones we have used in the past (e.g., Klos et al., 2018; Klos et al., 2023), which have become standard preliminary analysis steps over recent years. We then classify vertical displacements

https://doi.org/10.5194/essd-2026-469
Preprint. Discussion started: 10 July 2026

across Europe as reliable for use in hydrogeodetic studies. To this end, we use the methodology presented in Klos et al. (2023), which involves decomposing series into three predefined temporal scales: short-term, seasonal, and long-term, and correlating these decomposed time series with a high-resolution hydrological model described in *Section 2.2* at the corresponding temporal scale. In detail, the following steps are taken:

1. We use daily vertical displacements observed by 6,259 GPS stations over Europe. We perform a detailed manual check of the vertical displacement time series and select time series for at least 1 year as sufficient for further analysis, i.e., we retain 80% of time series at this stage. It is worth mentioning that only 60 of these stations have a length of less than 3 years. We further reject stations with many missing values, many outliers, and multiple offsets that cannot be explained by physical phenomena and may arise from station-dependent effects or unknown and unexplained reasons. We complete this step with 4,443 stations.
2. We remove outlying values by applying the three-times the interquartile range (IQR) rule.
3. We perform an iterative manual check of offsets over three iteration rounds. We start by using the offset database provided by NGL and then perform a manual check of the time series. We estimate and apply additional offsets that are visible in the time series but have not been reported by NGL. We also remove epochs for which an offset has been registered in the NGL-provided database, but no change is visible in the time series. In the case of offsets occurring during a break in the time series, we compare the mean values of the time series before and after the break. We determine the amplitudes of offsets by including all identified epochs to a full deterministic model, as proposed in Bogusz and Klos (2016), and then correct the time series.
4. We remove the impact of non-tidal atmospheric and non-tidal oceanic loading on the GPS-observed displacements by removing the daily model-predicted displacements. We retrieve publicly available loading correction products from the German Center for Geoscience (GFZ; Dill and Dobslaw, 2013) which use the ECMWF atmospheric surface pressure and simulated bottom pressure fields from the Max-Planck-Institute for Meteorology Ocean Model (MPIOM). We interpolate these predictions using the bilinear interpolation to GPS locations prior to correction.
5. We remove the effect of post-glacial rebound using the glacial isostatic adjustment model ICE6G-D (Stuhne and Peltier, 2015; Peltier et al., 2018) by interpolating the gridded predictions of vertical displacements to GPS locations and further removing these from the GPS-observed vertical displacements.
6. We complete the pre-processing procedure with 4,443 clean time series of GPS vertical displacements.
7. We estimate and subtract the linear trend from the daily displacement time series.
8. We fill in the gaps in the trend-corrected time series using linear interpolation.
9. We extrapolate the time series five years back and five years forward to reduce edge effects in the next step, using a deterministic harmonic regression model that includes trend, annual, semi-annual, and ordinary white noise components.
10. We apply forward wavelet transformation and reconstruction of wavelet coefficients using Meyer's mother wavelet, which guarantees no loss of information (Meyer, 1990), to decompose the time series into 9 levels. The number of levels into which we divide the series is determined by the daily sampling interval of the displacements and the periods of the signals we want to obtain.
11. We form a short-term signal containing signal variation at temporal scales ranging from 2 days to 5 months by summing the detail levels 1-6.
12. A seasonal signal containing signal variation at temporal scales ranging from 4 months to 1.4 years is retrieved by summing detail levels 7 and 8.

https://doi.org/10.5194/essd-2026-469
Preprint. Discussion started: 10 July 2026

13. A long-term signal containing signal variation at temporal scales above 1.1 years is retrieved by summing the remaining components. Note that the long-term signal does not include the linear trend, which was removed in *Step 7*.
14. We cut off the extrapolated epochs.
15. We cut out the interpolated epochs.
16. We apply the same procedure, i.e., *Steps 7-15*, to the high-resolution vertical displacements predicted from the hydrological model CLM5.0 (see *Section 2.2*).
17. We compare the time coverage between the GPS-observed displacements with that predicted by the model and include only stations with coverage greater than 1 year. This stage reduces the number of stations to 4,117.
18. We correlate the displacement time series observed by GPS and predicted from the hydrological model, separately at each temporal scale (short-term, seasonal, long-term).
19. We include those stations in the GPS benchmark dataset whose time series correlate significantly and positively with the high-resolution hydrological model using different classification thresholds: correlations higher than 0.3 and statistically significant for long-term and seasonal temporal scales; correlations higher than 0.1 and statistically significant for short-term temporal scales. The threshold for p-value is 0.05 in all cases.
20. The above steps lead to the following number of stations classified as reliable for hydrogeodetic analysis: 2,329 stations for the short-term temporal scale, 3,401 stations for the seasonal temporal scale and 2,521 stations for the long-term temporal scale (Klos and Bogusz, 2026).

2.4 Methods and data used for regional validation of benchmark datasets

To validate the provided GPS benchmark datasets, but also to present their extreme consistency and usefulness, we compare them with a range of external datasets. We provide (1) a region-wise qualitative assessment, (2) a quantitative assessment, and (3) a preliminary analysis of their significance for future estimates of TWS changes for different temporal scales using the inversion approach. We present analyses (2) and (3) for the Seine River Basin with an area of 78,500 km², where ongoing climate change is leading to more severe droughts: The latest report by the Organization for Economic Cooperation and Development (OECD) (March 2025) indicates that the Paris metropolitan area must respond effectively to growing water shortages, as it may not be able to meet its water demand over the next few decades (OECD, 2025).

2.4.1 Qualitative validation of benchmark datasets

We perform a qualitative assessment of GPS benchmark datasets for GPS locations divided into 11 regions. The division of stations is based on the parameters of the stochastic part of the displacement time series, i.e., stations classified into one region are characterized by a similar amplitude of power-law noise and a similar spectral index determined with maximum likelihood estimation method (see Supplementary Materials for more details). We average the signals regionally separately for each temporal scale and compare them with three external datasets described below. All three datasets are divided into three temporal scales to be consistent with the GPS-observed displacements included in the benchmark datasets.

1. We use a gravity field solution derived from the Satellite Laser Ranging (SLR) and the Doppler Orbitography and Radiopositioning Integrated by Satellites (DORIS) data (Löcher et al., 2025; Löcher and Kusche, 2021). These spherical harmonic time series were estimated based on satellite tracking data to up to 16 satellites, observed by SLR or DORIS techniques. The SLR and DORIS monthly gravity models have been available since 1984; they are characterized by a GRACE-like spatial resolution (Löcher et al., 2025; Löcher and Kusche, 2021), which is, however, not free of spatial constraints since in this solution leading empirical orthogonal functions from the GRACE era have been fitted to the raw

https://doi.org/10.5194/essd-2026-469
Preprint. Discussion started: 10 July 2026

tracking data. We compute vertical displacements at GPS locations from the spherical harmonic coefficients complete to degree and order 60. To estimate the vertical displacements at the GPS location, we use the same forward load modeling as described in *Section 2.2*.

2. We use monthly land-surface precipitation data provided by the Global Precipitation Climatology Centre (GPCC) and we further transform them to accumulated precipitation dataset. The dataset is available from January 1891 to December 2020. This data is based on historical rain gauge records from approximately 86,000 stations worldwide, collected via the Global Telecommunication System (GTS) and other historical sources (Schneider et al., 2022).
3. We use soil moisture provided by the European Centre for Medium-Range Weather Forecasts (ECMWF). Soil moisture fields are simulated with the land surface component of the ECMWF Integrated Forecasting System (HTESSEL scheme), which accounts for precipitation, evaporation, runoff, infiltration, and soil hydraulic processes. We use layers of monthly volumetric soil water parameters representing the fraction of water volume relative to soil volume within predefined soil layers. We use four vertically stratified soil layers up to 289 cm depth from 1995 available on 0.1° per 0.1° grid. The final soil moisture value is calculated as a weighted average based on the thickness of each soil layer.

2.4.2 Quantitative validation of benchmark datasets

To assess the GPS benchmark datasets quantitatively, we produce a high-resolution spatiotemporal vertical land-motion (VLM) map for the Seine River Basin by processing 848 Sentinel-1A SAR acquisitions from two ascending tracks between June 2, 2017 to March 2, 2024 provided by the Alaska Satellite Facility (ASF, 2024) using the WabInSAR algorithm (Shirzaei and Bürgmann, 2017; Shirzaei, 2023; Lee and Shirzaei, 2023). Interferograms are generated with the GAMMA software (Werner, 2000) using a maximum temporal baseline of 350 days and a perpendicular baseline of 35 m, yielding an average ground resolution of 78 m after incorporating permanent and distributed scatterers following Lee and Shirzaei (2023), which has been shown to be consistent with GPS. Line-of-sight (LOS) displacement time series, rates and their standard deviations are estimated for each pixel via least-squares optimization in a local reference frame. The resulting temporal sampling rate of the time series varies between 5 and 19 days, with a median of 7 days. Further details on InSAR processing are provided in Table S1 in SM. LOS velocities were then converted to vertical land motion assuming that deformation is dominated by the vertical component, which is valid given the absence of active faults or major earthquakes in northern France during the observation period, using $VLM_i = LOS_i / \cos\theta_i$. VLM fields from the two tracks are mosaicked into a seamless regional map following Ojha et al. (2018). Finally, we apply an affine transformation to convert the spatiotemporal VLM results into the IGS14 global reference frame (Ohenhen et al., 2023; Blackwell et al., 2020), consistent with GPS-observed vertical displacements we use, incorporating the global VLM model of Hammond et al. (2021). We interpolate InSAR-derived displacements into daily samples, to be temporarily consistent with those observed by GPS, and average them within the radius of 200 m around the GPS station. We then divide the InSAR-derived vertical displacements into three temporal scales, using the same methodology we apply for the GPS-observed displacements. We then compare the Euclidean distances between GPS-observed and InSAR-derived displacements across these three temporal scales and compute correlation coefficients between the displacement time series.

2.4.3 TWS recovery over Seine River Basin

We use the three benchmark datasets in the Seine River Basin, i.e., 190, 281, and 246 stations, respectively, for the short-term, seasonal and long-term temporal scales, and invert the daily vertical displacements to obtain TWS changes for 1,656 grid nodes at a spatial resolution of 0.25° per 0.25° following the methodology presented by Argus et al. (2014) and Fu et al. (2015). Seine River Basin extends from 0.3°E to 5.6°E and from 47.0°N to 50.0°N. However, to avoid a so-called “edge effect” (Fu et al., 2015), we extend this area into 2.375°W to 8.875°E longitude and 44.125°N to 52.875°N latitude.

https://doi.org/10.5194/essd-2026-469
Preprint. Discussion started: 10 July 2026

We validate our GPS-inverted TWS changes using TWS changes estimated from the GRACE mass concentration blocks (mascons) provided by the Jet Propulsion Laboratory (JPL) as RL06.3_v04 solution (Watkins et al., 2015; Wiese et al., 2016; Landerer et al., 2020). In the JPL mascon solution, the C20 and C30 parameters are replaced with satellite laser measurement results, as described in Technical Note TN-14 (Loomis et al., 2020). The degree-1 coefficients are estimated using the methods from Sun et al. (2016). GIA effect has been removed based on the ICE6G-D model from Peltier et al. (2018). We use GRACE TWS changes from 2002 to 2023.

We also use TWS changes from the fifth-generation of European ReAnalysis (ERA5) provided by the ECMWF (Muñoz Sabater, 2019; Copernicus Climate Change Service, 2022). We use the monthly averages of the volumetric soil water layer (VSWL; 1-4 layers summed: 0-289 cm) and snow water equivalent (SWE) for the period April 2002 to May 2022 and combine them to derive the ERA5-Land TWS on a 0.1° per 0.1° grid. We then interpolate these TWS change estimates linearly to a 0.25° per 0.25° grid to keep consistency with the GPS-inverted TWS grid.

TWS estimates derived from GRACE and ERA5-Land are divided into three temporal scales to keep consistency with the GPS benchmark datasets; all are then averaged over the Seine River basin.

2.4.4 Comparison of trends

We use the same monthly TWS changes observed by GRACE gravity mission as in the previous section. We also use monthly TWS changes in a global grid with a size of 0.5° per 0.5°, provided within the Global Land Water Storage dataset release 2 (GLWS2.0, Gerdener et al., 2023a, 2023b). GLWS is produced by assimilating gridded GRACE TWS anomalies into the WaterGAP global hydrological model. GLWS-predicted TWS changes thus represent groundwater, soil moisture, and surface water changes and are provided for the 2003-2020 time period.

We transform these GRACE- and GLWS-like gridded TWS changes into spherical harmonic coefficients following Wahr et al. (1998) approach. We convert GRACE-derived TWS changes to the degree and order equal to 120, representing the resolution of mass concentration blocks (Save et al., 2016; Scanlon et al., 2016), and GLWS-predicted TWS changes to the degree and order equal to 360, which represents the nominal resolution of the model, i.e., 0.5°. Then, we apply load Love numbers derived from the Gutenberg-Bullen A Earth model and methodology given by Farrell (1972) to estimate the vertical displacements for GPS locations for 221 and 204 months, respectively, for GRACE and GLWS. We then estimate linear trends for all displacement time series by fitting a simple deterministic model, consisting of trend, annual, and semi-annual components, into all the time series. We note here that the values of trends of the JPL GRACE mascon solution of most large-scale effects are similar between this solution and solutions based on spherical harmonic coefficients (Watkins et al., 2015); however, mascon solutions provide significantly better resolution for small-scale signals. It is also worth noting that trends observed via GPS encompass all phenomena, including local land subsidence, whereas trends derived from GRACE data and forecasted by GLWS reflect only hydrological loading. It is also worth noting that GPS-observed trends include local ground subsidence, while GRACE-derived and GLWS-predicted trends represent hydrospheric loading only.

3 Results and discussion

Below, in the following subsections, we present comprehensive comparisons of our GPS benchmark datasets with various external datasets.

3.1 Qualitative assessment

We now compare the GPS-observed displacements, classified as the benchmark dataset at the long-term temporal scale at the regional level, with the external datasets described in *Section 2.4.1*.

https://doi.org/10.5194/essd-2026-469
Preprint. Discussion started: 10 July 2026

Scandinavia (included in region 1 in Fig. 2) experienced several wet seasons, i.e., 1994-1995, 1999-2001, 2005-2006, 2010, and 2012, and two dry seasons in 2006-2007 and 2019-2020. The largest and first flood in Sweden occurred in the Glomma and Logan river basins in 1995, when previous maximum discharge records were exceeded by as much as 60% at gauging sites (Arheimer and Lindström, 2015). This effect is clearly visible in GPS-observed displacements, with a 3 mm difference between 1994 and 1996. The following years were wet periods with increased precipitation in 1998, 2000, 2005, 2008, 2010, and 2012, for which Spinoni et al. (2015) found total drought indices over 1.4, indicating severely wet conditions. These wet periods coincide with GPS-observed displacement changes in the range of ±2 mm. For the first part of the period analyzed, GPS-observed displacements are delayed with respect to soil moisture records of approximately 100 days; however, after 2010, both series match each other well, with the maximum value of soil moisture in 2012. We also notice an increase in precipitation for all these periods to 50 mm/month. The second pre-GRACE wet period, lasting from 1999 to 2001, is very well captured by GPS-observed displacements; we observe a distinct reduction in GPS displacements, but this is not reflected in the water storage maps derived from SLR and DORIS tracking data. The dry period of 2006-2007, which caused a decline in streamflow in Sweden, are also clearly visible in GPS-observed displacements through a sharp uplift of about 1.5 mm but are not evident in the water storage records derived from SLR and DORIS tracking data. We also observe the lowest precipitation level during this period. For the second dry period in 2018-2019, classified as an agricultural drought (Ducros et al., 2025), GPS-observed displacements increased sharply by 1 mm. This is confirmed by a drop in soil moisture below -30 mm and by the water storage maps derived from SLR and DORIS tracking data.

In region 2, two major floods caused by heavy rainfall occurred in 2004-2005 and 2017-2018 (e.g., https://www.ilmateenistus.ee/). Both periods were recorded as decreases in GPS-observed displacements of up to -2.5 mm. Precipitation dropped in 2006 to about 22% of the average level (Ingver et al., 2010), which is indicated by soil moisture values below -40 mm. For GPS-observed displacements, we observe an uplift of 4 mm, confirming dry conditions.

Region 3 experienced five dry periods in 2003, 2007, 2008, 2009, and 2010 (Walz et al., 2018), all of which were caused by extremely high temperatures (Semenova and Vicente-Serrano, 2024). These periods are captured in GPS-observed displacements; we notice a distinct increase of displacements during dry events. These dry periods are also well reflected in the soil moisture changes. We observe decreases in GPS-observed displacements below -3 mm in 2003-2009 and 2016-2020, which coincide with several extreme precipitation events in Ukraine since 2000 (Agayar et al., 2024). These phenomena are also well captured by the water storage maps derived from SLR and DORIS tracking data, for which we observe a sharp decline in displacements in 2003 that corresponds exactly to the decline in GPS-observed displacements. Subsequently, a slow return to normal conditions is observed for both displacements. GPS-observed displacements decrease again in 2016, but this is not recorded by the displacements derived from the water storage values derived from SLR and DORIS records. GPS displacements may reflect an increase in precipitation, which reaches values above 100 mm/month since 2016.

Region 4 mainly covers Turkey. Turkey has experienced alternating wet and dry periods. Dry periods occurred in 1998-2000, 2007, and 2020, while wet periods occurred in 2003-2007 and 2014-2015. The drought that affected Turkey in 1998 was probably the worst drought in the eastern Mediterranean region in the last nine centuries (Cook et al., 2016). After the drought, we see a decrease in GPS-observed displacements and a wet period from 2003 to 2007. This period is clearly visible in GPS-observed displacements and is also well reflected in the soil moisture values and in water storage records from SLR and DORIS. All datasets remain consistent until 2007, when a dry period occurs, as reflected in GPS-observed displacements and soil moisture decreases by 0.05 m^3/m^3, but not fully captured by water storage from SLR and DORIS. This drought is obviously captured by GPS-observed displacements as an increase of almost 5 mm and by the GRACE drought index determined by Khorrami and Gündüz (2022). It correlates well with low precipitation during this period and maximum values of the NAO (North Atlantic Oscillation) index (Cook et al., 2016). The displacements predicted from water storage values based on SLR and DORIS data do not reflect these dry conditions. After this drought, we see a decrease in GPS-

https://doi.org/10.5194/essd-2026-469
Preprint. Discussion started: 10 July 2026

observed displacements and a wet period from 2003 to 2007. This period is distinctly visible in GPS-observed displacements and is also well reflected in water storage maps from SLR and DORIS. All these datasets are consistent until 2007, when a dry period occurs, well reflected in the displacements observed by GPS, but not fully captured by SLR and DORIS-based water storage. Further, we observe a decrease in GPS-observed displacements in 2019, which is not captured by water storage from SLR and DORIS. It may be related to an increase in precipitation compared to the last few years (Bulut and Sakalli, 2021).

Region 5 covers mainly Bulgaria. For Bulgaria, we observe a surprisingly long-term consistency between GPS-observed displacements and displacements predicted from water storage based on SLR and DORIS data as well as the soil moisture values. This is clearly visible for the period 2000-2006, when all data present a marked decline, indicating a long-term drought. Soil moisture values do not compare well with GPS-observed displacements until 2000. Subsequently, all values increase, but until the end of the analyzed period, all three series are very consistent with each other. Flooding in 2005-2006 is associated with precipitation above average (Micheva et al., 2020) and overlaps with maximum soil moisture values around 0.1 m^3/m^3. A few periodic flash floods driven by torrential rains occurred in 2014-2019 (Micheva et al., 2020). The increase in GPS-observed displacements from 1997-1998 to 5 mm may reflect a meteorological drought in South Bulgaria (Stoyanova and Nikolova, 2022), which is not observed in other datasets.

Region 6 experiences alternating periods of extreme weather conditions. Wet periods occurred in 1996-1997, 2009-2011, and 2013-2017, while dry periods occurred in 1998-2008, 2012, and since 2019. Events up to 2012 coincide with periods indicated by Spinoni et al. (2015), who pointed out heavy rainfall and heat waves. These are clearly visible in GPS-observed displacements, especially events prior to 2000, when displacements vary by ±5 mm. These events are also recorded by SLR and DORIS tracking data. We note a significant decrease in values across all datasets during the 2009-2011 rainy period that also overlaps with maximum soil moisture values around 0.7 m^3/m^3. Between 2013 and 2017, we notice changes in GPS displacements, which may be caused by massive flooding resulting from overflowing the northern Italian rivers (Ojeda et al., 2022). In 2017, some parts of Italy were the driest in 60 years, with rainfall 80% below average (Blauhut et al., 2022). This is reflected in a 3 mm decrease in GPS-observed displacements and soil moisture values close to 0.03 m^3/m^3 at the beginning of 2017.

Three wet periods were reported for region 7, namely: 1997, 2002, 2010, and two dry periods: 2015, 2019-2020. However, severe and extreme meteorological drought conditions already prevailed also for the pre-GRACE period, in 1994-1995 (Kalbarczyk and Kalbarczyk, 2022), and these are perfectly reflected by GPS-observed displacements, which increase at that period to the values of almost 5 mm. They also correspond to lower precipitation levels during this period. This drought is, however, not reflected by the water storage maps derived from SLR and DORIS records. Region 7 is characterized by floods caused by successive waves of intense rainfall. This led to a series of floods in Poland in 1997, when rivers overflowed throughout the country (Kundzewicz et al., 1999), and in 2010 in southern Poland (Wilk and Kinal, 2014). Both floods are distinctly visible as a decrease in GPS-observed displacements during those periods. Both periods are also reflected well in the soil moisture values, increasing to 100 mm in 2010. Displacements predicted from water storage based on SLR and DORIS data reflect only the second flood period in 2010, during which they decrease below -2.5 mm. In recent years, Poland has also experienced several extreme and severe droughts, e.g., in 2018-2019 and in the spring of 2020 (Pinskwar et al., 2020). They are recorded in GPS-observed displacements as a decrease of more than 2 mm. They are also clearly reflected by soil moisture values, which are around 0.08 m^3/m^3 during that time.

Region 8 covers most of Germany. Two wet periods were recorded for this region, namely 1994-1996 and 2011-2012, associated with a series of storms, and three dry periods in 1996, 2002-2004 and 2018-2019 associated either with rainfall deficits or high temperatures (e.g., Spinoni et al., 2015; Blauhut et al., 2022; Boeing et al., 2024). The 2004 dry period is reflected by soil moisture values below -0.07 m^3/m^3. Both floods are perfectly captured by GPS-observed displacements; we note their decreases during those periods to -2.5 mm. The second flood period, i.e., 2011-2012, is also well captured by the

https://doi.org/10.5194/essd-2026-469
Preprint. Discussion started: 10 July 2026

water storage maps from SLR and DORIS records, but soil moisture is slightly delayed. There are also two significant long-term decreases in GPS-observed displacements during 1997-2002 and 2011-2016, not previously reported as wet periods. A large-scale European drought in 2018-2019 in Germany, associated with soil moisture drought, is also observed in the GPS-observed displacements, but delayed; we observe a decrease in GPS-observed displacements in winter 2019-2020. This drought is captured by the soil moisture dataset, whose values are below -0.1 m^3/m^3, and by the increase of displacements predicted from water storage maps based on SLR and DORIS, up to 2.5 mm.

For region 9, two events were recorded before 2000, namely the drought in 1995-1996 and the flood in 1997. The drought was caused by heat waves in 1995, which was the third hottest year since 1659 (Marsh, 1996). It is clearly visible in GPS-observed displacements, which have increased significantly in subsequent years and exhibit minimum soil moisture values in 1995. The 1997 flood was caused by two successive waves of intense rainfall, which caused rivers across the UK to burst their banks (Sibley, 2017). This phenomenon is captured by GPS-observed displacements, which decreased to below -2 mm. However, this phenomenon is not captured by displacements predicted from water storage values based on SLR and DORIS records. Soil moisture values increase abruptly from -0.05 m^3/m^3 to 0.02 m^3/m^3 for one year. Dry conditions have dominated this region in 2004-2005, 2012, and 2019. The lack of precipitation caused an intense drought in Western Europe, which is associated with a positive NAO index (García-Herrera et al., 2007). GPS-observed displacements and displacements predicted from SLR and DORIS do not reflect these phenomena. Subsequent droughts in the region are driven by significant temperature anomalies across the country (e.g., Turner et al., 2021) and coincide with estimates of the combined climate index (Spinoni et al., 2015). Finally, the recent increase in GPS-observed displacements and those predicted from SLR and DORIS water storage maps observed in 2022 is related to drought in this region.

Region 10, mainly covering France, experiences extreme weather events almost every 3-4 years. Wet periods were recorded for this region in 1994, 2000-2001, 2003, 2007-2008, 2010, 2012-2016, 2018-2019, and 2021, and dry periods in 1996-1998, 2006-2007, 2011, and 2017. All of them are clearly visible in the decreases and increases in GPS-observed displacements, precipitation, and the minimum and maximum values of soil moisture. Displacements predicted by SLR and DORIS are also well correlated with other datasets over time.

Region 11, covering Spain, has experienced periods of severe drought lasting at least two years in 1997-1998, 2003-2007, 2011-2012, 2017-2018, and 2022-2023, and two wet periods in 1996-1997 and 2013-2017. All these phenomena were caused by rising temperatures, and changes in precipitation, as well as other phenomena such as cyclones (e.g., Spinoni et al., 2015; Berbel and Esteban, 2019). During these periods, also high variations in precipitation, between 50 and 100 mm/month can be noticed. In 2004-2005, the precipitation was less than 60% of the average precipitation, and Spain experienced at that time one of the worst droughts that were ever recorded (García-Herrera et al., 2007). This period of drought is well captured by GPS-observed displacements, which rise up to 2 mm at that time, and a drop in soil moisture below -0.06 m^3/m^3. It is not captured, however, by water storage maps derived from SLR and DORIS data. The period between 2013 and 2017 was characterized by record-breaking rainfalls, which hit Spain and led to flash floods with maximum anomalies in 2013, early 2015, and 2017 (Berbel and Esteban, 2019). These periods of wet conditions are well captured by GPS-observed displacements, whose values decrease steadily until 2017. We observed maximum values of soil moisture in 2013, and then systematic increases until the 2017 drought. Afterwards, they start to increase as the period changes into a dry one. For the pre-GRACE period, GPS-observed displacements exceed 5 mm, indicating dry conditions between 1995 and 1996. This is confirmed by a low precipitation level near 50 mm/month and soil moisture values around -0.08 m^3/m^3, but is not captured by the displacements predicted from SLR and DORIS.

It is worth noting that for each of the regions presented in Fig. 2, we also include the number of GPS stations that were active during each time period. For all regions, the years 1994–2005 are characterized by moderate station activity, while

https://doi.org/10.5194/essd-2026-469
Preprint. Discussion started: 10 July 2026

after 2005 the number of stations increased sharply. This will certainly contribute to more reliable estimates of average displacements within a given region and improve the quality of the hydrosphere information provided.

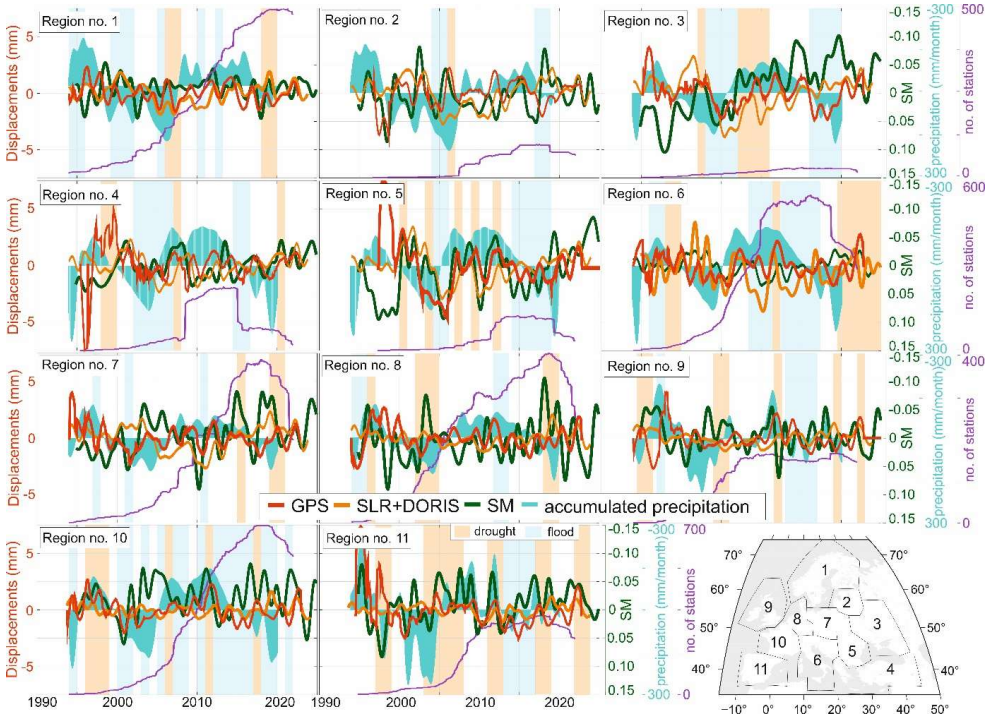

Figure 2: Comparison of GPS-observed displacements with soil moisture (SM), accumulated precipitation and displacements derived from water storage maps based on SLR and DORIS tracking data (SLR+DORIS); all are estimated for GPS locations. All estimates are then stacked and averaged within regions presented on the map. The comparison is presented for the long-term temporal scale. We also add the number of GPS stations that were active during the individual epochs.

3.2 Quantitative assessment

We now present a quantitative validation of GPS vertical displacements. For this, we use GPS stations located in the Seine River basin, which we classified as a benchmark dataset (Fig. 3). This set consists of 190, 281, and 246 stations, respectively, for the short-term, seasonal, and long-term temporal scales. We also use the displacements determined by the InSAR technique for the GPS locations, described in *Section 2.4.2*.

We observe very good consistency between the GPS-observed and InSAR-derived displacements across all three temporal scales, as confirmed by relatively low Euclidean distances (Figure 3 b, c, d), with median values equal to 169 mm, 167 mm, and 156 mm, respectively, for the short-term, seasonal and long-term temporal scales. For stations located in the eastern part of the Seine River basin, approximately 10% of the benchmarked stations, the Euclidean distances increase to 500 mm for the long-term and seasonal temporal scales and to 300 mm for the short-term temporal scale. This may be due to the locations of GPS stations in less urbanized, more vegetated regions. Seasonal vegetation growth and changes in canopy structure reduce InSAR coherence and introduce temporal decorrelation. This decorrelation increases phase noise in InSAR time series, leading to higher variability (standard deviation) compared to GPS-observed displacements, which are not affected by vegetation-induced scattering. The increased variability in the InSAR signal therefore primarily reflects vegetation-related decorrelation rather than deficiencies in other processing components, such as orbit or atmospheric corrections.

https://doi.org/10.5194/essd-2026-469
Preprint. Discussion started: 10 July 2026

Open Access Earth System Science Data Discussions

For the correlation coefficients (Figure 3 e, f, g), we observe excellent agreement between GPS-observed and InSAR-derived displacements at seasonal temporal scale. In contrast, at long-term temporal scale, the relationship is less consistent, and the agreement of the displacement time series varies across stations. We observe lower correlation between InSAR-derived and GPS-observed displacements at short-term temporal scale. This reduced correlation is consistent with the generally higher variability of InSAR-derived displacements compared to GPS across all temporal scales analyzed, likely reflecting the higher noise level and lower short-term stability of InSAR measurements, as well as additional noise contributions that vary across different satellite flight paths.

It should be further considered that the two techniques do not measure exactly the same physical quantity: InSAR captures the vertically integrated surface deformation signal, including deep, shallow, and surficial processes, whereas GPS sensors might be anchored to monument depths and may not fully reflect near-surface effects such as thermal expansion, shallow sediment compaction or hydro-compaction, for example, which can also explain some of the discrepancies, especially in the short-term and long-term temporal scales.

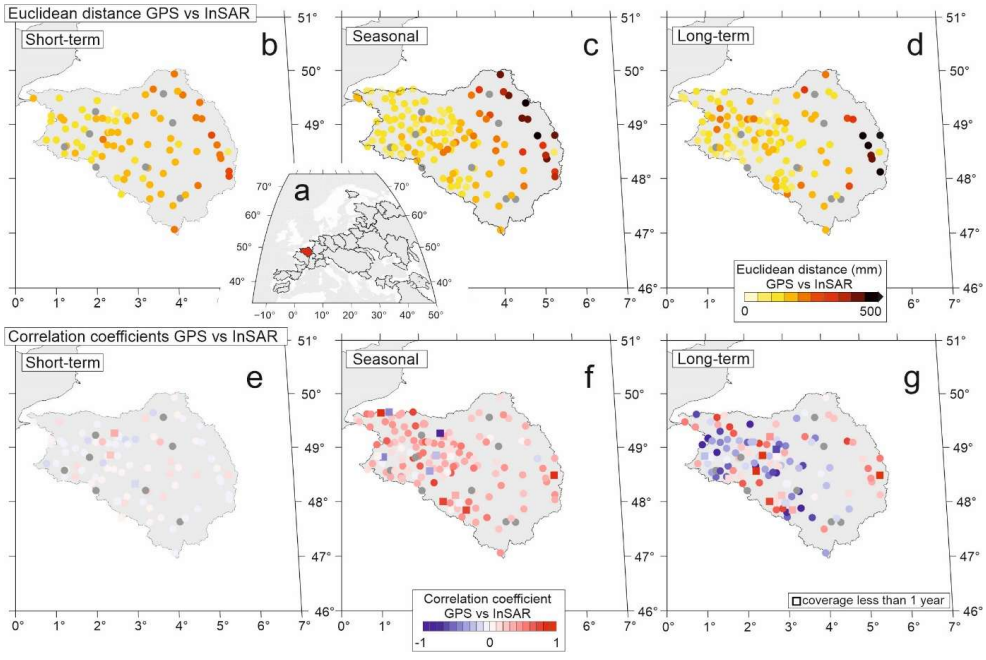

Figure 3: Comparison between daily GPS-observed displacements classified as benchmark datasets and daily-interpolated InSAR-derived displacements evaluated at GPS locations at three temporal scales within the Seine river basin located in western Europe (a). Shown are the Euclidean distances (in mm) (b-d) and correlation coefficients (e-g) between displacement time series from GPS and InSAR (evaluated at the GPS locations).

3.3 TWS change estimates over the Seine River Basin

We estimate GPS-inverted TWS for the Seine River Basin and compare it with external TWS datasets, for all three temporal scales, as described in *Section 2.4.3*. We observe perfect agreement among all three datasets at the seasonal temporal scale for the 2012-2016 period (Fig. 4), both for the amplitude and the phase of the seasonal signal. Prior to 2012, GPS-inverted TWS values are larger than those estimated using GRACE and the ERA5-Land model. This may be due to the smaller number of GPS displacement time series available during this period, which affects the reliability of TWS. Poorer GPS-inverted TWS estimates are also evident for this period for both short-term and long-term temporal scales. For the period after 2016, GPS-

https://doi.org/10.5194/essd-2026-469
Preprint. Discussion started: 10 July 2026

inverted TWS agrees with GRACE-derived TWS for the seasonal temporal scale, and both slightly deviate from the ERA5-Land estimates. This may be related to the fact that groundwater is not well represented in ERA5-Land, and its usage in this region is large. We also observe very good agreement between all three TWS change estimates on the long-term temporal scale. GPS-inverted TWS change follows increases and decreases in TWS changes observed by GRACE and predicted by the ERA5-Land model. For short-term temporal scales, the agreement between all three estimates is the worst. GPS-inverted TWS has the largest standard deviation for this temporal scale, much larger than the standard deviations of the TWS estimated from GRACE and the TWS predicted from the ERA5-Land model. However, by comparing results presented in Fig. 4a to those shown in Figs. 4b-d, we clearly see that our benchmarking approach allows us to reduce noise on long-term and seasonal temporal scales and to extract smaller-scale hydrospheric signals more reliably from the GPS-observed displacement time series. As mentioned before, we expect that the quality of GPS-observed displacements on a short-term temporal scale will certainly improve in the future by applying better background models, which will further enhance their relevance in the research on hydrosphere.

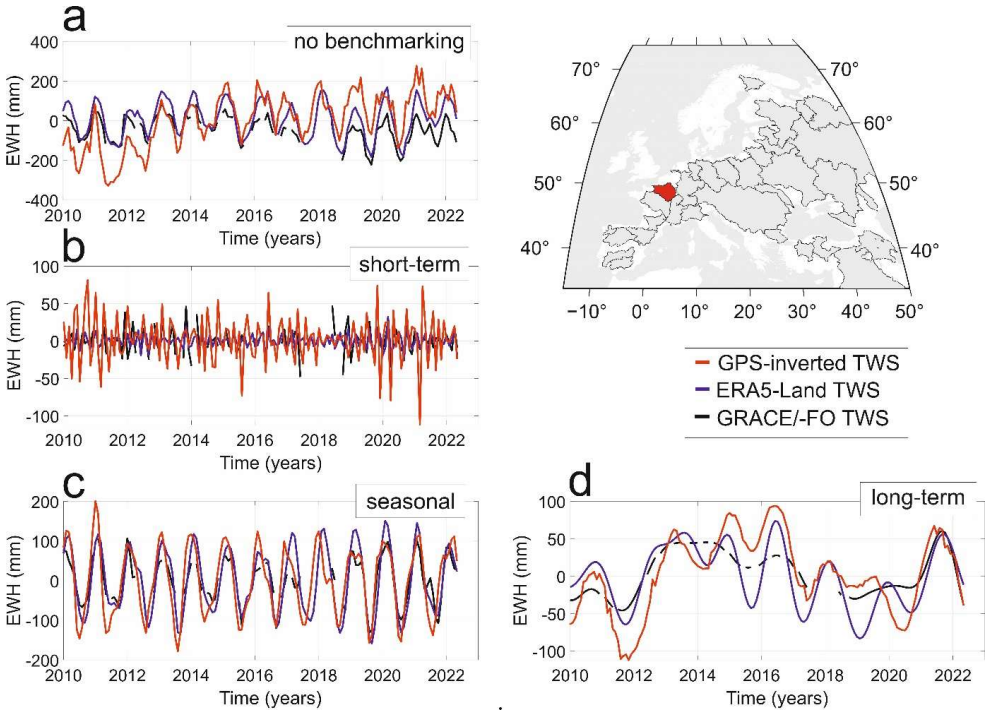

Figure 4: TWS changes for the Seine River Basin, a comparison of averaged TWS changes between GPS-inverted TWS, ERA5-Land-predicted TWS and GRACE-derived TWS. In the latter two cases, the TWS changes are estimated for GPS locations and then averaged for the entire catchment area. (a) TWS changes for the original set of GPS displacements, without classification of GPS stations. (b-d) TWS changes are estimated based on GPS-observed displacements for the benchmark dataset within three temporal scales: short-term, seasonal, and long-term.

3.4 GPS-observed trends and validation

Now, we provide a comprehensive description of GPS-observed, GRACE-derived and GLWS-predicted linear trends. These values are estimated for the GPS vertical displacements in *Step 7* and removed from the time series. Caution should be taken when using them in hydrogeodesy, as they are estimated based on different time intervals corresponding to the period during which the station was operational, in contrast to GRACE-derived and GLWS-predicted trends, whose values are estimated for

https://doi.org/10.5194/essd-2026-469
Preprint. Discussion started: 10 July 2026

the same period. With this in mind, we decided to conduct an additional analysis, presented below, which outlines trends across different time periods, by extracting the same time intervals from GPS, GRACE, and GLWS.

3.4.1 Trends over the entire period from 1994 to 2023

Figure 5 presents the vertical land motion trends estimated for 4,443 GPS locations using GPS-observed (after removing GIA), GRACE-derived and GLWS-predicted vertical displacements. The linear trends derived from GRACE indicate a steady uplift of the European region with a uniform value, not exceeding 0.5 mm/yr. Greater uplift can be observed in the eastern regions of Europe, but even there it does not exceed 1 mm/yr. These results confirm a clear continent-wise decline in TWS values, caused by recent prolonged droughts driven by climate change. The phenomenon of increasing losses in water storage across the continent, i.e., the drying tendency of Europe, measured by the GRACE mission, was quantified by Chandanpurkar et al. (2025). Vertical land motion linear trends predicted by GLWS confirm that several areas of Europe are indeed experiencing an uplift, which may be related to their drying. In Central Europe, this may be related to changes in atmospheric circulation (Bestakova et al., 2024). In the Paris Basin, this is due to recent droughts and increasing water scarcity, which are critical problems in the region, especially in the context of altered precipitation patterns caused by climate change (OECD, 2025). In the Alps, this may be due to severe snow shortages and rapid melting of snow and glaciers caused by a heat wave (NOAA, 2025). Sweden is experiencing a trend toward warmer temperatures and increased humidity, with some regions affected by complex phenomena such as droughts and heatwaves, or droughts and floods (Passos et al., 2024). However, it should be noted that in the Fennoscandian region, a strong uplift effect, even if it has already been subtracted with GIA model, may leave its fingerprint in the time series. Italy is facing its worst drought in two centuries, on an unprecedented scale, which has led, among other things, to the drying up of Italy's longest river, the Po (Montanari et al., 2023). The forecasts are not optimistic, as they indicate that the average TWS and extreme TWS will decrease significantly in this region in the future (Rezaei et al., 2024). The Venetian Delta is sinking dramatically due to natural sediment compaction and historical groundwater extraction, compounded by sea-level rise (Anzidei et al., 2025). Southern Spain is facing a serious water crisis due to expanding irrigated agriculture (Junquera et al., 2025). Several regions across Europe appear in GLWS as subsiding. These have been also been identified by Gerdener et al. (2023a).

The vertical land motion trends observed using GPS are roughly consistent with what we see in the GLWS predictions. The drying of Central Europe, Sweden, the Alps, the Mediterranean regions, Spain, the Paris basin and Italy is clearly visible. The United Kingdom and Ireland are also drying, in line with Antwi et al. (2022). Several individual trends appear to be outlying from the regional patterns. GPS trends estimated for several regions are negative and do not agree with GRACE estimates of continental drying. These are regions of Spain, France, Venice, UK, eastern Poland, Bulgaria and Turkey. There are also some alternating individual negative and positive trends found in Greece, and this may be related to tectonic activity in this region (Papanikolaou et al., 2025).

We also compare vertical land motion trends estimated from GPS-observed displacements estimated for two time periods, i.e., 1994-2003 and 2002-2023; the latter coincides with the period covered by the GRACE mission. We observed only minor differences between the two estimates.

3.4.2 Evolution of trends over years

Figure 6 shows the linear trends in vertical land motion estimated from 4,443 vertical displacements observed by GPS and derived from GRACE for four periods: 2003-2005, 2005-2010, 2010-2015, and 2015-2020. We note, however, that we use only vertical displacements observed by GPS for which we have more than 80% of observations in a given period. Since the number of stations has changed over the years, we have a different number of stations for each period.

https://doi.org/10.5194/essd-2026-469
Preprint. Discussion started: 10 July 2026

For the first period, i.e., 2003-2005, trends derived from GRACE indicate slight subsidence in the European region. Greater subsidence occurred in Scandinavia, but it did not exceed 1 mm/yr. However, trends observed by GPS for this period do not indicate subsidence of the European region. We observe clear uplifts in Central Europe and Scandinavia, exceeding 1 mm/yr in extreme cases. Trends observed by GPS indicate clear subsidence in the Rhine and Danube river basins and in areas around the Adriatic Sea.

For the second period, i.e., 2005-2010, GRACE trends show a slight uplift of the European region, not exceeding 1 mm/yr. Trends recorded by GPS show significant uplift in the Scandinavian region, exceeding 1.5 mm/yr, and significant uplift in the Italian region, exceeding 2 mm/yr. We also observe several alternating spatial patterns of uplift and subsidence in Central Europe. However, these are difficult to identify due to the high variability of trends between individual stations.

For the third period, i.e., 2010-2015, we observe a striking similarity between the trends observed by GPS and those derived from GRACE, with clear spatial patterns, consistent between both datasets. We observe clear subsidence in Spain, northern Italy, the United Kingdom, and France, with subtle trends derived from GRACE and much larger, but still negative, trends observed by GPS. Central Europe is characterized by positive trends derived from GRACE and positive trends derived from GPS. For Iceland, we observe clear uplift for both datasets. The only difference between the GPS and GRACE trends is the Scandinavian region, where, based on GRACE trends, we observe subsidence in its southern part and uplift in the northern part. In the case of GPS trends, we observe evident uplifts across almost the entire Scandinavian region.

For the most recent period, i.e., 2015-2020, GRACE-derived trends show subtle uplift across Europe, with values not exceeding 0.5 mm/yr. We observe slight subsidence in southern Italy and the Balkan countries. GPS-observed trends indicate an apparent uplift of Scandinavia, with values exceeding 1 mm/yr. Central Europe is also experiencing local uplifts. Southern Italy is undergoing significant subsidence, with values below -1 mm/yr.

Dividing the period from 1994 to 2023 into sub-periods does indeed bring benefits when interpreting long-term changes. However, these sub-periods may absorb changes on a multi-year scale, which are included in the long-term temporal scale of the benchmark datasets. For this reason, we do not provide them separately, but we do show their consistency with the GRACE and GLWS trends over the years. We observe a continuous, clear uplift in Iceland, as the trends have been consistent over the years. In this region, excessive ice melting has been observed, causing the Earth's surface to uplift (e.g., Auriac et al., 2013). Obviously, a continuous residual uplift in Scandinavia can be observed from mismodelling of GIA effect. The subsidence affects areas of Spain, France, UK, Italy, Poland, Turkey, Romania, and Bulgaria. It partly coincides with the trends estimated from GRACE for the 2010-2015 period, although the scale of this subsidence is much smaller for GRACE. This subsidence coincides with the regions indicated by Herrera-Garcia et al. (2021) to be threatened by land subsidence caused by the depletion of groundwater. This is a slow process that develops over a long period of time, causing the Earth's surface to gradually subside, even by decimeters per year, usually over very large areas (Herrera-Garcia et al., 2021).

For several regions, trends vary from period to period; for example, in central Italy, we see alternating positive and negative trends over the years. We observed a similar pattern along the coasts of Spain and Portugal.

https://doi.org/10.5194/essd-2026-469
Preprint. Discussion started: 10 July 2026

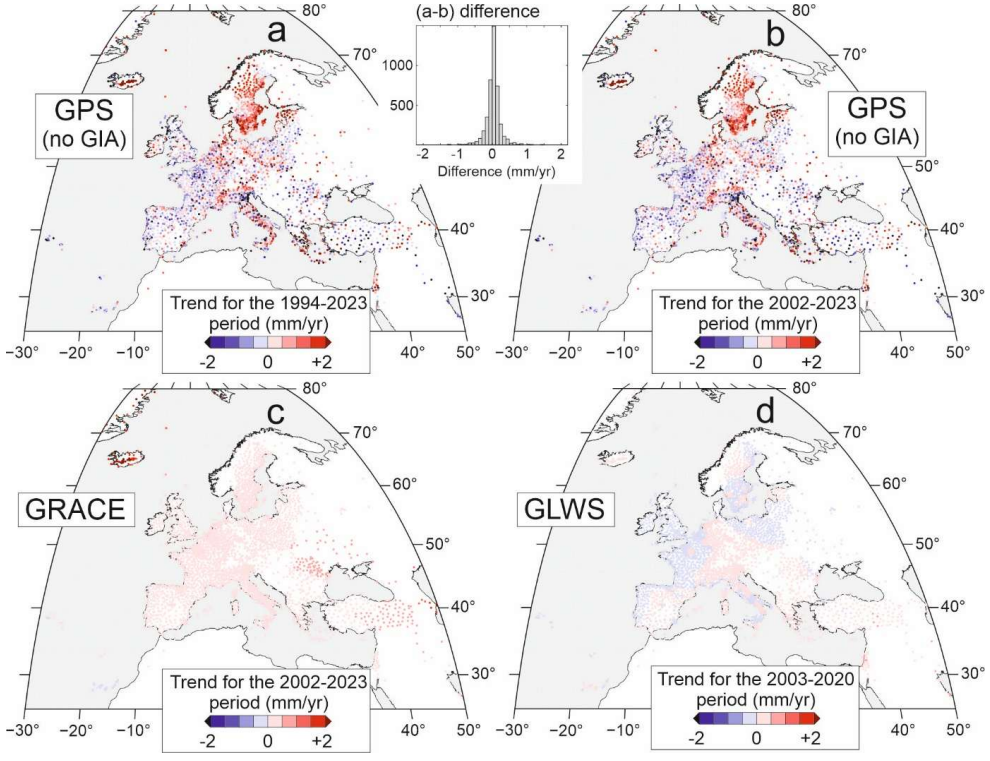

570 **Figure 5: Linear trends estimated for 4,443 GPS locations based on GPS-observed (a, b), GRACE-derived (c), and GLWS-predicted (d) vertical displacements. Note that the GPS trends (a, b) are after subtracting the effect of GIA. (a) shows GPS trends for the entire period of station operation between 1994 and 2023, while (b) shows GPS trends for the period consistent with GRACE, i.e., 2002-2023.**

https://doi.org/10.5194/essd-2026-469
Preprint. Discussion started: 10 July 2026

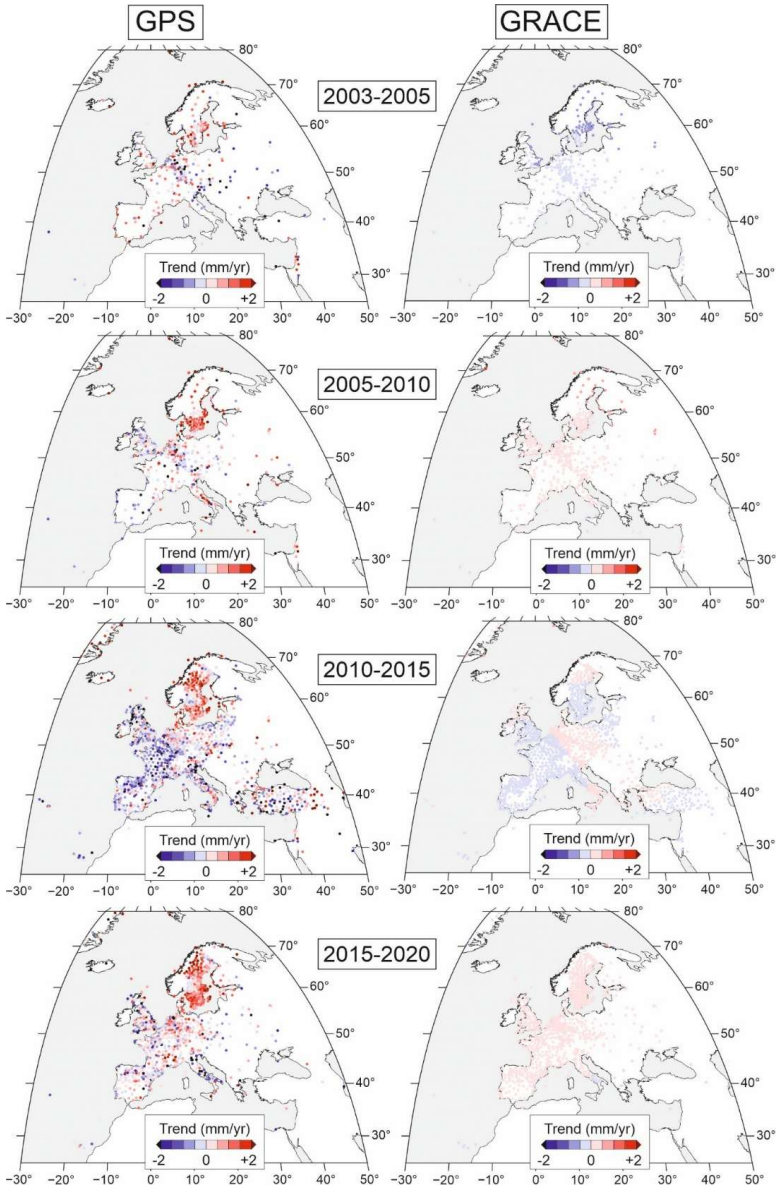

575 **Figure 6: Trends of vertical displacements from 4,443 stations we use for benchmarking. Trends are presented for 4 different time periods, but only for stations whose observations cover at least 80% of the period considered. Left column: trends estimated from GPS-observed vertical displacements (GIA removed), right column: trends estimated from GRACE-derived vertical displacements, estimated for GPS locations.**

4 Summary

580 For the first time, we present three quality-controlled and cleaned datasets of vertical daily GPS displacements from 1994 to 2023 time span, applicable to analyses of changes in the hydrosphere in Europe. Datasets allow for the reliable analyses of long-term, seasonal and short-term changes and are provided according to the GPS benchmarking procedure presented in Klos et al. (2023). It is clear that this approach allows us to significantly reduce noise on long-term and seasonal temporal scales, as well as to better extract small-scale hydrospheric signals.

https://doi.org/10.5194/essd-2026-469
Preprint. Discussion started: 10 July 2026

585 Our datasets of GPS vertical displacements show clear temporal agreement with hydrological signals, particularly with seasonal wet and dry cycles. Benchmarking of the displacements allows to reliably distinguish responses to precipitation events between regular seasonal cycles and long-term signals that are related to climate variability and groundwater changes. The strong agreement between GPS-observed displacements and InSAR-, SLR+DORIS-, GRACE-derived displacements, as well as between GPS-inverted TWS and TWS for ERA5-Land, and GRACE data demonstrates the reliability of our approach.

590 GPS-observed displacements can serve as a valuable, independent tool for monitoring hydroclimatic conditions, making them highly relevant for water management applications, detection of drought onset, duration, and recovery, as well as can support more informed decision-making in water resource allocation, reservoir management, and agricultural planning. In the future, the European GPS network may also serve as operating system for TWS estimates.

595 **Data availability**

The benchmark datasets of GPS stations may be accessed at: https://repod.icm.edu.pl/dataset.xhtml?token=39effba4-57eb-4109-911e-f7d15ff65cbc and should be cited as Klos and Bogusz (2026).

GPS daily time series are provided by NGL through: http://geodesy.unr.edu/. eCLM data are available through: https://detect-z03.geoinformation.net/geonetwork/srv/eng/catalog.search#/metadata/18fd2642-02bc-4096-a600-1993fdfdc346.

600 GRACE/GRACE-FO mascon data (JPL RL06.3_v04) are available at: http://grace.jpl.nasa.gov. GPCC data are available online at https://opendata.dwd.de/climate_environment/GPCC/html/download_gate.html. SWI climate index is available through: https://confluence.ecmwf.int/display/CEMS/Model+Output. ERA5-Land TWS is downloaded from: https://cds.climate.copernicus.eu/. The GLWS2.0 dataset is downloaded from: https://doi.pangaea.de/10.1594/PANGAEA.954742. The river basins boundaries are downloaded from:
605 https://www.hydrosheds.org/. Maps are drawn using the Generic Mapping Tools software (Wessel et al. 2019).

Supplement link

The supplementary material is provided as separate file and published with this article.

Author contributions

Conceptualization: AK, JK, JB. Data curation: AK, AS, AL, JM, YE, CM, SW, JB. Formal analysis: AK, AS, AL, JM, JR,
610 KK, YE, CM, SW, JB. Funding acquisition: AK, JK. Investigation: AK, AS, AL, JM, YE, CM. Methodology: AK, JK, AS, AL, SW, JB. Software: AK, AS, AL. Validation: AK, AL, JM, JR, KK, MS. Visualization: AK, AL. Writing (original draft preparation): AK. Writing (review and editing): All.

Competing interests

The authors declare that they have no conflict of interest.

615 **Financial support**

The research is supported by the National Science Centre, Poland, grant no UMO-2022/45/B/ST10/00333. JK, AS and YE acknowledge funding by the Deutsche Forschungsgemeinschaft (DFG, German Research Foundation)—SFB 1502/1-2022—

https://doi.org/10.5194/essd-2026-469
Preprint. Discussion started: 10 July 2026

Project No. 450058266. JK and CM acknowledge funding by DFG in the framework of the project SLRDORISDA (KU 1207/42-1).

References

Adusumilli, S., Borsa, A. A., Fish, M. A., McMillan, H. K., and Silverii, F.: A decade of water storage changes across the contiguous United States from GPS and satellite gravity. Geophys. Res. Lett., 46, 22, 13006–13015. https://doi.org/10.1029/2019GL085370, 2019.

Agayar, E., Aemisegger, F., Armon, M., Scherrmann, A., and Wernli, H.: Precipitation extremes in Ukraine from 1979 to 2019: climatology, large-scale flow conditions, and moisture sources. Nat. Hazards Earth Syst. Sci., 24, 7, 2441-2459, https://doi.org/10.5194/nhess-24-2441-2024, 2024.

Antwi, S.H., Rolston, A., Linnane, S., and Getty, D.: Communicating water availability to improve awareness and implementation of water conservation: A study of the 2018 and 2020 drought events in the Republic of Ireland. Sci. Total Environ., 807, 2, 150865, https://doi.org/10.1016/j.scitotenv.2021.150865, 2022.

Anzidei, M., Tolomei, C., Trippanera, D., Alberti, T., Bosman, A., Brunori, C.A., Serpelloni, E., Vecchio, A., Falciano, A., and Deli, G.: Multi-Temporal Relative Sea Level Rise Scenarios up to 2150 for the Venice Lagoon (Italy). Remote Sens., 17, 820, https://doi.org/10.3390/rs17050820, 2025.

Argus, D.F., Fu, Y., and Landerer, F.W.: Seasonal variation in total water storage in California inferred from GPS observations of vertical land motion. Geophys. Res. Lett., 41, 6, 1971–1980, https://doi.org/10.1002/2014GL059570, 2014.

Arheimer, B., and Lindström, G.: Climate impact on floods: changes in high flows in Sweden in the past and the future (1911–2100). Hydrol. Earth Syst. Sci., 19, 2, 771–784, https://doi.org/10.5194/hess-19-771-2015, 2015.

ASF, Copernicus Sentinel data. Retrieved from Alaska Satellite Facility (ASF) DAAC on March 8, 2024, at https://search.asf.alaska.edu, processed by ESA, 2024.

Auriac, A., Spaans, K.H., Sigmundsson, F., Hooper, A., Schmidt, P., and Lund, B.: Iceland rising: Solid Earth response to ice retreate inferred from satellite radar interferometry and viscoelastic modeling. J. Geophys. Res. Solid Earth, 118, 1331-1344, https://doi.org/10.1002/jgrb.50082, 2013.

Berbel, J., and Esteban, E.: Droughts as a catalyst for water policy change. Analysis of Spain, Australia (MDB), and California. Glob. Environ. Change, 58, 101969, https://doi.org/10.1016/j.gloenvcha.2019.101969, 2019.

Bestakova, Z., Kysely, J., Lhotka, O., Heilig, M., and Eitzinger, J.: Warm-season drying across Europe and its links to atmospheric circulation. Earth Space Sci., 11, 6, e2023EA003434, https://doi.org/10.1029/2023EA003434, 2024.

Blackwell, E., Shirzaei, M., Ojha, C., and Werth, S.: Tracking California's sinking coast from space: implications for relative sea-level rise. Sci. Adv., 6, eaba4551, https://doi.org/10.1126/sciadv.aba4551, 2020.

Blauhut, V., Stoelzle, M., Ahopelto, L. et al.: Lessons from the 2018–2019 European droughts: a collective need for unifying drought risk management. Nat. Hazards Earth Syst. Sci., 22, 6, 2201–2217, https://doi.org/10.5194/nhess-22-2201-2022, 2022.

Blewitt, G., Hammond, W.C., and Kreemer, C.: Harnessing the GPS data explosion for interdisciplinary science. Eos, 99, https://doi.org/10.1029/2018EO104623, 2018.

Boening, F., Wagener, T., Marx, A., Rakovec, O., Kumar, R., Saaniego, L., and Attinger, S.: Increasing influence of evapotranspiration on prolonged water storage recovery in Germany. Environ. Res. Lett., 19, 2, https://doi.org/10.1088/1748-9326/ad24ce, 2024.

https://doi.org/10.5194/essd-2026-469
Preprint. Discussion started: 10 July 2026

655 Bogusz, J., and Klos, A.: On the significance of periodic signals in noise analysis of GPS station coordinates time series. GPS Solut., 20, 4, 655-664, https://doi.org/10.1007/s10291-015-0478-9, 2016.

Bulut, U., and Sakalli, A.: Impacts of climate change and distribution of precipitation on hydroelectric power generation in Turkey. IOP Conference Series Materials Science and Engineering, 1032, 1, 012043, https://doi.org/10.1088/1757-899X/1032/1/012043, 2021.

660 Carlson, G., Werth, S., and Shirzaei, M.: Joint inversion of GNSS and GRACE for Terrestrial Water Storage Change in California. J. Geophys. Res. Solid Earth, 127, 3, e2021JB023135, https://doi.org/10.1029/2021JB023135, 2022.

Carlson, G., Werth, S., and Shirzaei, M.: A novel hybrid GNSS, GRACE, and InSAR joint inversion approach to constrain water loss during a record-setting drought in California. Remote Sens. Environ., 311, 114303, https://doi.org/10.1016/j.rse.2024.114303, 2024.

665 Chandanpurkar, H.A., Famiglietti, J.S., Gopalan, K., Wiese, D.N., Wada, Y., Kakinuma, K., Reager, J.T., and Zhang, F.: Unprecedented continental drying, shrinking freshwater availability, and increasing land contributions to sea level rise. Sci. Adv., 11, 30, https://doi.org/10.1126/sciadv.adx0298, 2025.

Chen J., Cazenave A., Dahle C., Llovel W., and Panet I. et al.: Applications and Challenges of GRACE and GRACE Follow-On Satellite Gravimetry. Surv. Geophys., 43, 1, 305-345, https://doi.org/10.1007/s10712-021-09685-x, 2022.

670 Chew, C.C., and Small, E.E.: Terrestrial water storage response to the 2012 drought estimated from GPS vertical position anomalies. Geophys. Res. Lett., 41,6145–6151, https://doi.org/10.1002/2014GL061206, 2014.

Cook, B.I., Anchukaitis, K.J., Touchan, R., Meko, D.M., and Cook, E.R.: Spatiotemporal drought variability in the Mediterranean over the last 900 years. J. Geophys. Res. Atmospheres, 121, 5, 2060-2074, https://doi.org/10.1002/2015JD023929, 2016.

675 Copernicus Climate Change Service, ERA5-Land monthly averaged data from 1950 to present. Copernicus Climate Change Service (C3S) Climate Data Store (CDS), https://doi.org/10.24381/cds.68d2bb30 (Accessed on 30-06-2024), 2022.

Dill, R., and Dobslaw, H.: Numerical simulations of global-scale high-resolution hydrological crustal deformations. J. Geophys. Res. Solid Earth, 118, 9, 5008-5017, https://doi.org/10.1002/jgrb.50353, 2013.

Ducros, G., Tiggeloven, T., Ma, L., Daloz, A.S., Schuhen, N., Claassen, J., and de Ruiter, M.C.: Multi-hazards in Scandinavia:
680 impacts and risks from compound heatwaves, droughts and wildfires. Nat. Haz. Earth Syst. Sci., 25, 11, 4693-4712, https://doi.org/10.5194/nhess-25-4693-2025, 2025.

Eicker, A., Forootan, E., Springer, A., Longuevergne, L., and Kusche, J.: Does GRACE see the terrestrial water cycle "intensifying"?. J. Geophys. Res. Atmospheres, 121, 2, 733-745, https://doi.org/10.1002/2015JD023808, 2016.

Ewerdwalbesloh, Y., Montzka, C., Kusche, J., and Springer, A.: GRACE TWSA data assimilation in land surface models -
685 the role of state vector and model uncertainty representation. ESS Open Archive, https://doi.org/10.22541/essoar.175915589.90532565/v, 2026.

Farrell, W.E.: Deformation of the earth by surface loads. Rev. Geophys. Space Phys., 10, 761-797, 10.1029/RG010i003p00761, 1972.

Ferreira, V.G., Montecino, H.C., Ndehedehe, C.E., Heck, B., Gong, Z., de Freitas, S.R.C., and Westerhaus, M.: Space-based
690 observations of crustal deflections for drought characterization in Brazil. Sci. Total Environ., 644, 256–273, https://doi.org/10.1016/j.scitotenv.2018.06.277, 2018.

Fu, Y., Argus, D.F., and Landerer, F.W.: GPS as an independent measurement to estimate terrestrial water storage variations in Washington and Oregon. J. Geophys. Res. Solid Earth, 120, 1, 552–566, https://doi.org/10.1002/2014JB011415, 2015.

https://doi.org/10.5194/essd-2026-469
Preprint. Discussion started: 10 July 2026

García-Herrera, R., Hernández, E., Barriopedro, D., Paredes, D., and Trigo, R.M.: The Outstanding 2004/05 Drought in the Iberian Peninsula: Associated Atmospheric Circulation. J. Hydrometeor., 8, 3, 483-498, https://doi.org/10.1175/JHM578.1, 2007.

Gerdener, H., Kusche, J., Schulze, K., Doll, P., and Klos, A.: The global land water storage data set release 2 (GLWS2.0) derived via assimilating GRACE and GRACE-FO data into global hydrological model. J. Geod., 97, 73, https://doi.org/10.1007/s00190-023-01763-9, 2023a.

Gerdener, H., Schulze, K., and Kusche, J.: GLWS 2.0: A global product that provides total water storage anomalies, groundwater, soil moisture and surface water with a spatial resolution of 0.5° from 2003 to 2019 [dataset]. PANGAEA, https://doi.org/10.1594/PANGAEA.954742, 2023b.

Gobron, K., Rebischung, P., Chanard, K., and Altamimi, Z.: Anatomy of the spatiotemporally correlated noise in GNSS stations position time series. J. Geod., 98, 34, https://doi.org/10.1007/s00190-024-01848-z, 2024.

Gobron, K., Rebischung, P., Van Camp, M., Demoulin, A., and de Viron, O.: Influence of Aperiodic Non-Tidal Atmospheric and Oceanic Loading Deformations on the Stochastic Properties of Global GNSS Vertical Land Motion Time Series. J. Geophys. Res. Solid Earth, 126, 9, e2021JB022370, https://doi.org/10.1029/2021JB022370, 2021.

Gruszczynski, M., Klos, A., and Bogusz, J.: A Filtering of Incomplete GNSS Position Time Series with Probabilistic Principal Component Analysis. Pure Appl. Geophys., 175, 1841-1867, https://doi.org/10.1007/s00024-018-1856-3, 2018.

Hammond, W.C., Blewitt, G., Kreemer, C., and Nerem, R.S.: GPS Imaging of Global Vertical Land Motion for Studies of Sea Level Rise. J. Geophys. Res. Solid Earth, 126, 7, https://doi.org/10.1029/2021JB022355, 2021.

Han, S.-C., and Razeghi, M.: GPS Recovery of daily hydrologic and atmospheric mass variation: a methodology and results from the Australian Continent. J. Geophys. Res. Solid Earth, 122, 11, 9328-9343, https://doi.org/10.1002/2017JB014603, 2017.

Herrera-Garcia, G., Ezquerro, P., Tomas, R., et al.: Mapping the global threat of land subsidence. Sci., 371, 6524, 34-36, https://doi.org/10.1126/science.abb8549, 2021.

Humphrey, V., Rodell, M., and Eicker, A.: Using Satellite-Based Terrestrial Water Storage Data: A Review. Surv. Geophys., 44, 1489–1517, https://doi.org/10.1007/s10712-022-09754-9, 2023.

Ingver, A., Tamm, I, Tamm, U., Kangor, T, and Koppel, R.: The characteristics of spring cereals in changing weather in Estonia. Agronomy Research, 8(III), 533-562, 2010.

Jiang, W., Yuan, P., Chen, H., Cai, J., Li, Z., Chao, N., and Sneeuw, N.: Annual variations of monsoon and drought detected by GPS: A case study in Yunnan, China. Sci. Rep., 7, 5874, https://doi.org/10.1038/s41598-017-06095-1, 2017.

Jiang, Z., Hsu, Y.-J., Yuan, L., and Huang, D.: Monitoring time-varying terrestrial water storage changes using daily GNSS measurements in Yunnan, southwest China. Remote Sensing of Environment, 254, 112249, https://doi.org/10.1016/j.rse.2020.112249, 2021.

Junquera, V., Hormaza, J.I., Rubenstein, D.I., and Gavilan P.J.: Severe water crisis in southern Spain under expanding irrigated agriculture: A multidimensional drought analysis. Proc. Natl. Acad. Sci. U.S.A., 122, 39, e2508055122, https://doi.org/10.1073/pnas.2508055122, 2025.

Kalbarczyk, R., and Kalbarczyk, E.: Research into Meteorological Drought in Poland during the Growing Season from 1951 to 2020 Using the Standardized Precipitation Index. Agronomy, 12, 9, 2035, https://doi.org/10.3390/agronomy12092035, 2022.

https://doi.org/10.5194/essd-2026-469
Preprint. Discussion started: 10 July 2026

Khorrami, B., and Gündüz, O.: Detection and analysis of drought over Turkey with remote sensing and model-based drought indices. Geocartio International, https://doi.org/10.1080/10106049.2022.2066197, 2022.

Klos, A., and Bogusz, J. (2026): Benchmark datasets of vertical displacements of European GPS stations for hydrogeodesy, https://repod.icm.edu.pl/dataset.xhtml?token=39effba4-57eb-4109-911e-f7d15ff65cbc, dataset, RepOD.

Klos, A., Kusche, J., Leszczuk, G., Gerdener, H., Schulze, K., Lenczuk, A., and Bogusz, J.: Introducing the idea of classifying sets of permanent GNSS stations as benchmarks for hydrogeodesy. J. Geophys. Res. Solid Earth, 128, e2023JB026988, https://doi.org/10.1029/2023JB026988, 2023.

Klos, A., Olivares, G., Teferle, F.N., Hunegnaw, A., and Bogusz, J.: On the combined effect of periodic signals and colored noise on velocity uncertainties. GPS Solut., 22, 1, https://doi.org/10.1007/s10291-017-0674-x, 2018.

Kreemer, C., and Blewitt, G.: Robust estimation of spatially varying common-mode components in GPS time-series, J. Geod., 95, 13, https://doi.org/10.1007/s00190-020-01466-5, 2021.

Kundzewicz, Z.W., Szamalek, K., and Kowalczyk, P.: The Great Flood of 1997 in Poland. Hydrol. Sci. J., 44,6, 855-870, https://doi.org/10.1080/02626669909492285, 1999.

Landerer, F.W., Flechtner, F.M., Save, H., Webb, F.H., et al.: Extending the Global Mass Change Data Record: GRACE Follow-On Instrument and Science Data Performance. Geophys. Res. Lett., 47, 12, https://doi.org/10.1029/2020GL088306, 2020.

Langbein, J., and Svarc, J.L.: Evaluation of temporally correlated noise in global navigation satellite system time series: Geodetic monument performance. J. Geophys. Res. Solid Earth, 124, 1, https://doi.org/10.1029/2018JB016783, 2019.

Larochelle, S., Chanard, K., Fleitout, L., Fortin, J., Gualandi, A., Longuevergne, L., Rebischung, P., Violette, S., and Avouac, J.-P.: Understanding the Geodetic Signature of Large Aquifer Systems: Example of the Ozark Plateaus in Central United States. J. Geophys. Res. Solid Earth, 127, 3, e2021JB023097, https://doi.org/10.1029/2021JB023097, 2022.

Lau, N., Borsa, A.A., and Becker, T.W.: Present-Day Crustal Vertical Velocity Field for the Contiguous United States. J. Geophys. Res. Solid Earth, 125, 10, https://doi.org/10.1029/2020JB020066, 2020.

Lee, J.-C., and Shirzaei, M.: Novel algorithms for pair and pixel selection and atmospheric error correction in multitemporal InSAR. Remote Sens. Environ., 286, 113447, https://doi.org/10.1016/j.rse.2022.113447, 2023.

Lei, J., Chen, W., Li, Z., Li, F., and Zhang, S.: A Full-Spectrum Bedrock Thermal Expansion Model and Its Impact on the Global Positioning System Height Time Series. Geophys. Res. Lett., 47, 1, e2019GL086022, https://doi.org/10.1029/2019GL086022, 2020.

Lenczuk, A., Ndehedehe, C., Klos, A., and Bogusz, J.: A new multivariate drought severity index to identify short-term hydrological signals: case study of the Amazon River basin. Remote Sens. Environ., 315, 114464, https://doi.org/10.1016/j.rse.2024.114464, 2024

Loomis, B.D., Rachlin, K.E., Wiese, D.N., Landerer, F.W., and Luthcke, S.B.: Replacing GRACE/GRACE-FOC30 with satellite laser ranging: Impacts on Antarctic Ice Sheet mass change. Geophys. Res. Lett., 47, e2019GL085488, https://doi.org/10.1029/2019GL085488, 2020.

Löcher, A., and Kusche, J.: A hybrid approach for recovering high-resolution temporal gravity fields from satellite laser ranging. J. Geod., 95, 6, https://doi.org/10.1007/s00190-020-01460-x, 2021.

Löcher, A., Kusche, J., and Nie, Y.: A 40-year record of the Earth's time-variable gravity field from SLR and DORIS. Adv. Space Res., 76, 3, 1281-1291, https://doi.org/10.1016/j.asr.2025.05.089, 2025.

https://doi.org/10.5194/essd-2026-469
Preprint. Discussion started: 10 July 2026

Marsh, T.J.: Hydrological data United Kingdom. 1995 yearbook. Institute of Hydrology: British Geological Survey, 1996.

Meyer, Y.: Ondelettes et Opérateurs (Vol. I–III). Hermann, 1990.

Micheva, B., Tsekov, M., Meyer, U., Guerova, G.: Analysis of the 2014 Wet Extreme in Bulgaria: Anomalies of Temperature, Precipitation and Terrestrial Water Storage. Hydrol., 7, 3, 66, https://doi.org/10.3390/hydrology7030066, 2020.

Milliner, C., Materna, K., Bürgmann, R., Fu, Y., Moore, A. W., Bekaert, D., et al.: Tracking the weight of Hurricane Harvey's stormwater using GPS data. Sci. Adv., 4, 9, eaau2477, https://doi.org/10.1126/sciadv.aau2477, 2018.

Montanari, A., Nguyen, H., Rubinetti, S., Ceola, S., Galelli, S., Rubino, A., and Zanchettin, D.: Why the 2022 Po River drought is the worst in the past two centuries. Sci. Adv., 9, 32, https://doi.org/10.1126/sciadv.adg8304, 2023.

Muñoz Sabater, J.: ERA5-Land monthly averaged data from 1950 to present. Copernicus Climate Change Service (C3S) Climate Data Store (CDS), https://doi.org/10.24381/cds.68d2bb30 (Accessed on 30-06-2024), 2019.

NOAA National Centers for Environmental Information (NCEI), Global Drought Narrative, from https://www.ncei.noaa.gov, 2025.

OECD, Adapting the Paris Metropolitan Area to a Water-Scarce Future, OECD Publishing, Paris, https://doi.org/10.1787/00a103f8-en, 2025.

Ohenhen, L.O., Shirzaei, M., Ojha, C., and Kirwan, M.L.: Hidden vulnerability of US Atlantic coast to sea-level rise due to vertical land motion. Nat. Commun., 14, 2038, https://doi.org/10.1038/s41467-023-37853-7, 2023.

Ojeda, M.G.-V., Di Sante, F., Coppola, E., Fantini, A., Nogherotto, R., Raffaele, F., and Giorgi, F.: Climate change impact on flood hazard over Italy. J. Hydrol., 615, A, 128628, https://doi.org/10.1016/j.jhydrol.2022.128628, 2022.

Ojha, C., Shirzaei, M., Werth, S., Argus, D.F., Farr, T.G.: Sustained Groundwater Loss in California's Central Valley Exacerbated by Intense Drought Periods. Water Resour. Res., 54, 7, 4449–4460, https://doi.org/10.1029/2017WR022250, 2018.

Ouellette, K.J., de Linage, C., and Famiglietti, J.S.: Estimating snow water equivalent from GPS vertical site-position observations in the Western United States: SNOW water equivalent from GPS observations. Water Resour. Res., 49, 5, 2508–2518, https://doi.org/10.1002/wrcr.20173, 2013.

Papanikolaou, D., Nomikou, P., Lampridou, D., Preine, J., Litsas, D., Tsaparas, Y., Koliopanos, I., Petroulia, M., Huebscher, C.: Active faulting in Samos Basin, Eastern Aegean Sea, Greece and paleogeographic implications. Tectonophys., 905, 230724, https://doi.org/10.1016/j.tecto.2025.230724, 2025.

Passos, M.V., Kan, J.-C., Destouni, G., Barquet, K., and Kalantari, Z.: Identifying regional hotspots of heatwaves, droughts, floods, and their co-occurrences. Stoch. Environ. Res. Risk Assess., 38, 3875-3893, https://doi.org/10.1007/s00477-024-02783-3, 2024.

Peltier, W.R., Argus, D.F., and Drummond, R.: Comment on "An Assessment of the ICE-6G_C (VM5a) Glacial Isostatic Adjustment Model" by Purcell et al. J. Geophys. Res. Solid Earth, 123, 2019-2018, https://doi.org/10.1002/2016JB013844, 2018.

Pinskwar, I., Chorynski, A., and Kundzewicz, Z.W.: Severe Drought in the Spring of 2020 in Poland—More of the Same? Agron., 10, 11, 1646, https://doi.org/10.3390/agronomy10111646, 2020.

Poll, S., Rigor, P., Brdar, S., Ho-Hagemann, H.T.M., Hartick, C., van Hulten, M., Gonzalez-Nicolas, A., Keller, J., Caviedes-Voullieme, D., Hendricks-Franssen, H.-J., Goergen, K., and Kollet, S.: The new TSMP2 coupled Earth system model. EGUsphere [preprint], https://doi.org/10.5194/egusphere-2025-5468, 2025.

https://doi.org/10.5194/essd-2026-469
Preprint. Discussion started: 10 July 2026

Ray, J., Altamimi, Z., Collilieux, X., and van Dam, T.: Anomalous harmonics in the spectra of GPS position estimates. GPS Solut., 12, 55-64, https://doi.org/10.1007/s10291-007-0067-7, 2008.

Rezaei, A., Karami, K., Tilmes, S., and Moore, J.C.: Future water storage changes over the Mediterranean, Middle East, and North Africa in response to global warming and stratospheric aerosol intervention. Earth Syst. Dyn., 15, 1, https://doi.org/10.5194/esd-15-91-2024, 2024

Richter, H.M.P., Luck, C., Klos, A., Sideris, M.G., Rangelova, E., and Kusche, J.: Reconstructing GRACE-type time-variable gravity from the Swarm satellites. Sci. Rep., 11, 1117, https://doi.org/10.1038/s41598-020-80752-w, 2021.

Save, H., Bettadpur, S., and Tapley, B.D.: High-resolution CSR GRACE RL05 mascons. J. Geophys. Res., 121, 7547–5769, https://doi.org/10.1002/2016JB013007, 2016.

Scanlon, B.R., Zhang, Z., Save, H., Wiese, D.N., Landerer, F.W., Long, D., Longuevergne, L., and Chen, J.: Global evaluation of new GRACE mascons products for hydrologic applications. Water Resour. Res., 52, 9412-9429, https://doi.org/10.1002/2016WR019494, 2016.

Scanlon, B.R., Zhang, Z., Save, H., and Bierkens, M.F.P.: Global models underestimate large decadal declining and rising water storage trends relative to GRACE satellite data. Proc. Natl. Acad. Sci. U.S.A. 115, 6, E1080-E1089, https://doi.org/10.1073/pnas.1704665115, 2018.

Schneider, U., Hänsel, S., Finger, P., Rustemeier, E., and Ziese, M.: GPCC Full Data Monthly Product Version 2022 at 0.25°: Monthly Land-Surface Precipitation from Rain-Gauges built on GTS-based and Historical Data. https://doi.org/10.5676/DWD_GPCC/FD_M_V2022_025, 2022.

Semenova, I., and Vicente-Serrano, S.M.: Long-term variability and trends of meteorological droughts in Ukraine. Int. J. Climatol., 44, 6, 1849-1866, https://doi.org/10.1002/joc.8416, 2024.

Shirzaei, M.: A wavelet-based multitemporal DInSAR algorithm for monitoring ground surface motion. IEEE Geosci. Remote Sens. Lett., 10, 456–460, https://doi.org/10.1109/LGRS.2012.2208935, 2023.

Shirzaei, M., Bürgmann, R., and Fielding, E.J.: Applicability of Sentinel-1 terrain observation by progressive scans multitemporal interferometry for monitoring slow ground motions in the San Francisco Bay Area. Geophys. Res. Lett., 44, 2733–2742, https://doi.org/10.1002/2017GL072663, 2017.

Sibley, A.: Severe thunderstorm and flooding in East Devon on 7 August 1997. Weather. https://doi.org/10.1002/WEA.2935, 2017.

Spinoni, J., Naumann, G., Vogt, J.V., and Barbosa, P.: The biggest drought events in Europe from 1950 to 2012. J. Hydrol. Reg. Stud., 3, 509-524, https://doi.org/10.1016/j.ejrh.2015.01.001, 2015.

Springer, A., Mielke, C.A., Liu, Z., Dixit, S., Friederichs, P., and Kusche, J.: A regionally refined and mass-consistent atmospheric and hydrological de-aliasing product for GRACE, GRACE-FO and future gravity missions. J. Geophys. Res. Solid Earth, 129, 5, e2023JB027883, https://doi.org/10.1029/2023JB027883, 2024.

Stoyanava R., and Nikolova, N.: Meteorological drought in southwest Bulgaria during the period 1961-2020. J. Geogr. Inst. Cvijic, 72, 3, 243-255, https://doi.org/10.2298/IJGI2203243S, 2022.

Stuhne, G.R., and Peltier, W.R.: Reconciling the ICE-6G_C reconstruction of glacial chronology with ice sheet dynamics: The cases of Greenland and Antarctica. J. Geophys. Res. Earth Surf. 120, 1-25, https://doi.org/10.1002/2015JF003580, 2015.

https://doi.org/10.5194/essd-2026-469
Preprint. Discussion started: 10 July 2026

Sun, Y., Riva, R., and Ditmar, P.: Optimizing estimates of annual variations and trends in geocenter motion and J2 from a combination of GRACE data and geophysical models. J. Geophys. Res. Solid Earth, 121, 11, 8352-8370, https://doi.org/10.1002/2016JB013073, 2016.

Tapley, B.D., Bettadpur, S., Ries, J.C., Thompson, P.F., and Watkins, M.W.: GRACE measurements of mass variability in the Earth system. Sci., 305, 503, https://doi.org/10.1126/science.1099192, 2004.

Tapley, B.D., Watkins, M.M., Flechtner, F., et al.: Contributions of GRACE to understanding climate change. Nat. Clim. Change, 9, 358-369, https://doi.org/10.1038/s41558-019-0456-2, 2019.

Turner, S., Barker, L.J., Hannaford, J., Muchan, K., Parry, S., and Sefton, C.: The 2018/2019 drought in the UK: a hydrological appraisal. Weather, 76, 8, 248-253, https://doi.org/10.1002/wea.4003, 2021.

Wahr, J., Molenaar, M., and Bryan, F.: Time variability of the Earth's gravity field: hydrological and oceanic effects and their possible detection using GRACE. J. Geophys. Res., 103, 0205-30229, https://doi.org/10.1029/98JB02844, 1998.

Wahr, J., Khan, S.A., van Dam, T., et al.: The use of GPS horizontals for loading studies, with applications to northern California and southeast Greenland. J. Geophys. Res. Solid Earth, 118, 1795-1806, https://doi.org/10.1002/jgrb.50104, 2013.

Walz, Y., Dall, K., Graw, V., de Leon, J.-C.V., Haas, S., Kussul, N., and Jordaan, A.: Understanding and reducing agricultural drought risk: Examples from South Africa and Ukraine. Policy Report No. 3. Bonn: United Nations University – Institute for Environment and Human Security (UNU-EHS), 2018.

Watkins, M.M., Wiese, D.N., Yuan, D., Boening, C., Landerer, F.W.: Improved methods for observing Earth's time variable mass distribution with GRACE using spherical cap mascons. J. Geophys. Res. Solid Earth, 120, 4, 2648–2671, https://doi.org/10.1002/2014JB011547, 2015.

Werner, C. et al.: Gamma SAR and interferometric processing software. In *Proc. ERS-Envisat Symposium*, 2000.

White, A.M., Gardner, W.P., Borsa, A.A., Argus, D.F., and Martens, H.R.: A Review of GNSS/GPS in Hydrogeodesy: Hydrologic Loading Applications and Their Implications for Water Resource Research. Water Resour. Res., 58, 7, e2022WR032078, https://doi.org/10.1029/2022WR032078, 2022.

Wiese, D.N., Landerer, F.W., and Watkins, M.M.: Quantifying and reducing leakage errors in the JPL RL05M GRACE mascon solution. Water Resour. Res., 52, 9, 7490-7502, https://doi.org/10.1002/2016WR019344, 2016.

Wilk, S., and Kinal, J.: Flooding in Poland in 2010 as a Exemplification of Efforts of the Polish Social Work Services in Case of Disaster. Mediterr. J. Soc. Sci., 5, 13, https://doi.org/10.5901/mjss.2014.v5n13p315, 2014.

Yin, G., Forman, B. A., and Wang, J.: Assimilation of ground-based GPS observations of vertical displacement into a land surface model to improve terrestrial water storage estimates. Water Resour. Res., 57, e2020WR028763. https://doi.org/10.1029/2020WR028763, 2021.

Yin, G., Forman, B. A., Loomis, B. D., and Luthcke, S.B.: Comparison of vertical surface deformation estimates derived from space-based gravimetry, ground-based GPS, and model-based hydrologic loading over snow-dominated watersheds in the United States. J. Geophys. Res. Solid Earth, 125, 8, 1–19, https://doi.org/10.1029/2020JB019432, 2020.

Young, Z., Martens, H.R., Hoylman, Z.H., and Gardner, W.P.: Drought characterization with GPS: Insights into groundwater and surface-reservoir storage in California. Water Resour. Res., 60, 8, e2024WR037404, https://doi.org/10.1029/2024WR037404, 2024.

Zhan, W., Heki, K., Arief, S., and Yoshida, M.: Topographic amplification of crustal subsidence by the rainwater load of the 2019 typhoon Hagibis in Japan. J. Geophys. Res. Solid Earth, 126, 6, https://doi.org/10.1029/2021JB021845, 2021.

https://doi.org/10.5194/essd-2026-469
Preprint. Discussion started: 10 July 2026

Zumberge, J.F., Heflin, M.B., Jefferson, D.C., Watkins, M.M., and Webb, F.H.: Precise point positioning for the efficient and robust analysis of GPS data from large networks. J. Geophys. Res. Solid Earth, 102, B3, 5005-5017, https://doi.org/10.1029/96JB03860, 1997.